Classification of Low-Level Atmospheric Structures Based on a Pyramid Representation and a Machine Learning Method

Sebastián Sierra[2], Juan F. Molina[1], Angel Cruz-Roa[2], José Daniel Pabón[1,2,3], Raúl Ramos-Pollán[3], Fabio A. González[2], and Hugo Franco[1(✉)]

[1] Computer Engineering Department, Universidad Central, 110321 Bogotá D.C., Colombia
hfrancot@ucentral.edu.co
[2] MindLab Research Group, Universidad Nacional de Colombia, Ciudad Universitaria, 111321 Bogotá, Colombia
[3] Centre for Supercomputing and Scientific Computing, Universidad Industrial de Santander, Bucaramanga, Colombia

Abstract. The atmosphere is a highly complex fluid system where multiple intrinsic and extrinsic phenomena superpose at same spatial and temporal dominions and different scales, making its characterization a challenging task. Despite the novel methods for pattern recognition and detection available in the literature, most of climate data analysis and weather forecast rely on the ability of specialized personnel to visually detect atmospheric patterns present in climate data plots. This paper presents a method for classifying low-level wind flow configurations, namely: confluences, difluences, vortices and saddle points. The method combines specialized image features to capture the particular structure of low-level wind flow configurations through a pyramid layout representation and a state-of-the-art machine learning classification method. The method was validated on a set of volumes extracted from climate simulations and manually annotated by experts. The best results into the independent test dataset was 0.81 of average accuracy among the four atmospheric structures.

1 Introduction

The superposition of an intricate set of interactions between air, ocean and land components and states yields both regular (periodic or quasiperiodic) and chaotic patterns at different scales for atmospheric relevant variables –i.e. temperature, pressure, humidity, air velocity, density, chemical composition, etc. The dynamics of such patterns and their corresponding physical manifestations (cloud coverage, winds, rain, hail, snow, etc.) configure a continuous from climate (long time and space atmospheric scales) to weather (in short time scale and local domains).

Behind the specific occurrence of each observable atmospheric pattern, there are several physical processes converging at different spatial and temporal scales, determining their distinctive features. Indeed, the relevant structures for both

A. Pardo and J. Kittler (Eds.): CIARP 2015, LNCS 9423, pp. 19–26, 2015.
DOI: 10.1007/978-3-319-25751-8_3

climate and weather description are a compound of several atmospheric variable configurations present in a particular region at the same time.

Weather forecast is carried out by the coupling of mechanistic models, such as WRF (Weather Research and Forecasting Model [6]) and statistical processing of real data. Furthermore, computer simulations and data acquisition (satellite imagery, weather stations, RADAR) are just the first part of the process: a detailed empirical description from classical meteorological approaches allow specialists to visually detect atmospheric structures and manually track their evolution over time to *qualitatively* describe their dynamics and, then, predict the most probable scenarios according to each particular spatio-temporal configuration obtained [7]. Then, low level structure characterizations of the atmosphere are implicitly carried out by meteorologists on a daily basis, with the aid of computer systems that enhance data visualization (isolines, streamlines, data fusion on scalar and vector fields, etc.).

Moreover, the automatic detection of atmospheric structures, even for *low level* configurations (particularly, fluid flow patterns) is a challenging problem, given the high local and global variability of climatic data, no matter if it comes from experimental measurements or modeling and simulation results. Recent works are still exploring new techniques for structure representation and identification [4].

In the data visualization context, the works of Tzeng and Ma [10] and Gruchalla et al. [3] proposed frameworks for 3D fluid structure extraction and rendering by detecting regions of interests (ROIs) containing such patterns in the wavelet domain. Given that low level fluid structures are expected to have quite regular patterns, Rao et al. [9] presented a region-based detection and extraction method based in phase portraits, where the salient ROIs are those where the geometrical pattern of the vector field best matches the solution of the differential equation associated to the analytic structure description. Even the use of such methods in climate and weather data visualization, state of the art climate data analysis and weather forecast depends mainly on the ability and experience of the specialist to detect patterns constituting relevant atmospheric structures.

This work proposes a machine learning approach to support the automatic detection of such *low level* patterns, specifically those related to wind dynamics. The method takes as input a volume, which includes information of atmospheric variables (temperature, pressure, humidity and air velocity) at a given time in a particular region; next, different features based on divergence and curl differential operators are extracted from the volume represented as a spatial pyramid layout (SPL) and fed to a support vector machine classifier, which has been previously trained with a set of annotated volumes for four classes: confluence, difluence, vortex and saddle point (as it is shown in Figure 1); finally, the classifier outputs a prediction that indicates the probability of the presence of a particular low-level wind flow configuration. The method was evaluated over a set of volumes extracted from climate simulations and manually annotated by expert meteorologists.

The rest of paper is organized as follows: Section 2 explains the details of the proposed classification method. Section 3 describes the experimental evaluation –including the dataset description, the experimental setup and results–. Finally, Section 4 concludes with the main remarks and establishes the future work.

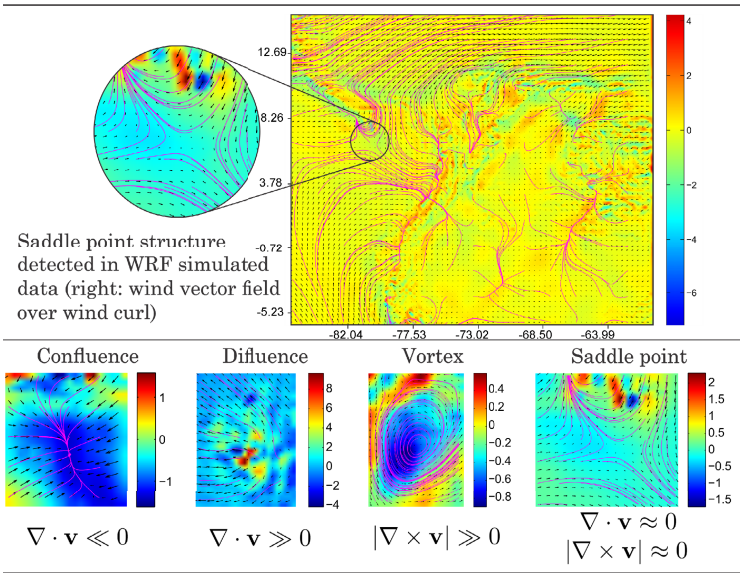

Fig. 1. Representative instances of confluence, difluence, vortex and saddle point wind structures in WRF simulated data for northern South America and the Caribbean. Winds (in m/s) are plotted over this geographical domain and its corresponding latitude and longitude coordinates (upper map) for a spatial resolution of 40 km.

2 Automatic Classification of *Low Level* atmospheric structures

An overview of the method herein proposed is depicted in Figure 2, which starts from a database of *low level* atmospheric structures manually annotated by experts meteorologists. For each annotated sample, an approximation of the differential operators curl and divergence is applied to capture characteristics of the wind velocity vector field into three atmospheric feature maps (curl, divergence, negative of divergence). Then, several histogram representations are built at different resolutions following a SPL. The final concatenation of the resulting histograms is used to train a machine learning classifier (support vector machine, SVM, or random forest, RF) to distinguish between four atmospheric structures (vortex, difluence, confluence and saddle point). The prediction is performed using the trained classifier over a particular ROI. The details of each step are presented in the following subsections.

2.1 Approximation of Differential Operators from Wind Velocity Field

Given $\nabla = \left(\frac{\partial}{\partial x}, \frac{\partial}{\partial y}\right)$ and $\mathbf{v} = (u, v)$, a vector field representing two dimensional components of winds *parallel* to Earth surface within an isobaric layer, it is

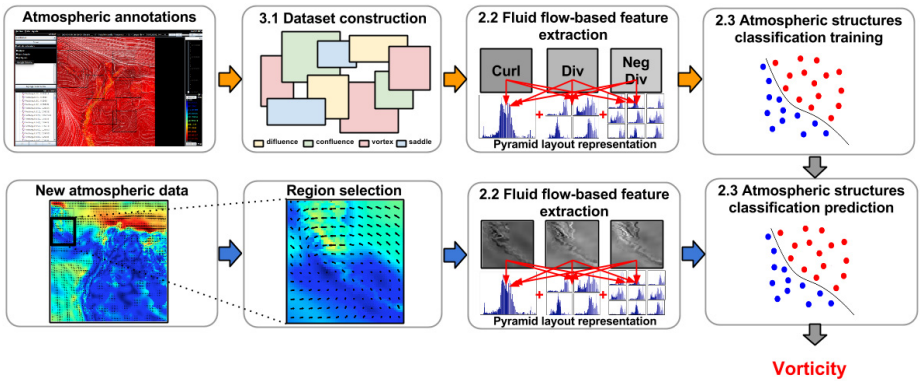

Fig. 2. Overall method description for automatic detection of atmospheric structures.

possible to derive expressions for both *divergence* and *curl* operators, to support further design of a fluid flow-based vector field descriptor. A simple discrete version of a two-dimensional $\mathbf{v}$, is the matrix $V = \{(u, v)_{ij}\}_{M \times N}$ where $i = 1, 2, \ldots, M$ is the index pointing to each row and $j = 1, 2, \ldots, N$ the index pointing to each column of the matrix.

Divergence. The divergence of $\mathbf{v}$ is defined as $\nabla \cdot \mathbf{v} = \frac{\partial u}{\partial x} + \frac{\partial v}{\partial y}$ for the two-dimensional case. Since this is an interior product, divergence is a scalar field. Using the basic centered finite difference approximation to each partial derivative, the 2D divergence can be estimated as $\nabla \cdot \mathbf{v} \approx {}^{(u_{i+1,j} - u_{i-1,j})}/_{2h} + {}^{(v_{i,j+1} - v_{i,j-1})}/_{2h}$.

Curl. The curl of a vector field determines how much the vectors within the dominion under study "rotate" around each particular position. In the 2D case, curl is easily build by taking into account only the rotation on the xy plane. Then $\nabla \times \mathbf{v} = \left(\frac{\partial v}{\partial x} - \frac{\partial u}{\partial y}\right) \bar{z}$, which, therefore, is always perpendicular to that plane and can be approximated by $\nabla \times \mathbf{v} \approx {}^{(v_{i+1,j} - v_{i-1,j})}/_{2h} - {}^{(u_{i,j+1} - u_{i,j-1})}/_{2h}$.

2.2 Fluid Flow-Based Feature Descriptor

Taking into account that an atmospheric structure can occur in different spatial locations and each phenomenon can have different scales, we propose a set of atmospheric-based feature descriptors able to support translational and scale invariance by using a SPL representation of the region of interest. Over the SPL, we extract features from the differential curl and divergence operators, max-pooling and the histogram of oriented optical flow as explained below.

Spatial Pyramid Layout (SPL) Representation. This representation allows to capture the atmospheric structures in different spatial locations and scales. As it is shown in Figure 3, the image is divided in different regions following a pyramidal layout organization. The first layer of the pyramid corresponds

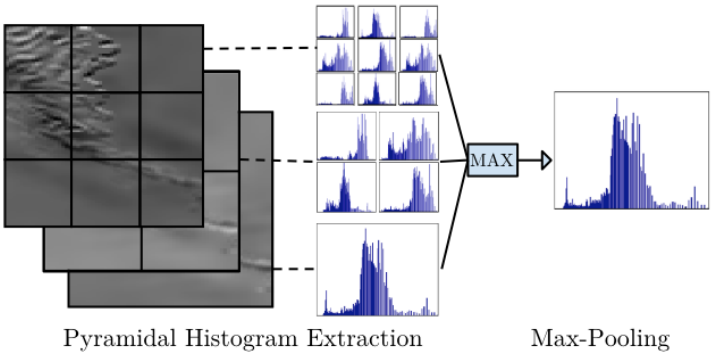

Fig. 3. Fluid flow-based feature descriptors. Histograms are extracted in a pyramid layout from the different feature maps. The resulting 14 histograms are further integrated in the max-pooling descriptor, which corresponds to a histogram with the maximum values for all the bins.

to the whole image, the second to a 2×2 division, and the third to a 3×3 division [5]. The image is represented by a concatenation of the resulting 14 normalized histograms for divergence, negative-divergence and curl feature maps.

Max-pooling. The max-pooling works to detect atmospheric structure independently of its location and scale. Max-pooling applies a maximum operator among the 14 histograms of all spatial layouts. This pooling function is typically used for detection tasks exploiting spatial invariances [8].

Histogram of Oriented Optical Flow. As a baseline, we decided to use histograms of oriented optical flow (HOOF) [2] attempting to detect the patterns in the wind flow that better describe each phenomena. Additionally, the SPL was also applied to this image representation.

2.3 Atmospheric Structure Classifier

For automatic prediction of the atmospheric structures, a Support Vector Machine (SVM) classifier and a Random Forest (RF) classifier were trained. For addressing the multiclass problem of classifying the atmospheric structures (vortex, difluence, confluence and saddle points), the SVM uses a one-vs-all strategy. The kernels evaluated for SVM were linear and radial basis function (RBF).

3 Experimental Evaluation

3.1 Atmospheric Structure Dataset Construction

The 4D (3D + time) data used in this study come from WRF regional climate simulations from the climate change study developed by Armenta and Pabón [1]

for the period between 1981 and 2010. These simulations were performed at a spatial resolution of $h = 10$ km and temporal resolution of 3 hours.

A monthly highest and lowest ocean surface temperature criterion was applied to focus on May and December data. An Extraction-Transformation and Load (ETL) process was performed to extract and transform to real units 3D fields for temperature, T, and wind velocity components, U, V and W, and then store them in raw files. For the region under study (northern South America and western Caribbean Sea), 27 isobaric slices were extracted, each of 287×280 uniform surface elements.

An annotation tool was developed specifically for these data. The tool loads simulation data and renders temperature and wind velocity for slices at different isobaric levels (up to 27 for each volume). Experts navigate the WRF data using the annotation software by exploring the 3D volumes along a specific time period, and are asked to manually segment the ROI containing one structure and to specify its particular type. The ROI bounding box is then stored in a XML file along with the corresponding class and related information, such as simulation time, isobaric level and divergence and rotational computations on the ROI. The resulting annotated dataset contains 793 annotations, 232 for confluences, 166 for divergences, 177 for saddles and 218 for vortices.

3.2 Experimental Design and Performance Measures

For evaluation purposes, we split the original dataset into two parts for training and testing. The testing dataset comprises a complete and independent 4D data from a simulation of a month with region annotations for all four climate phenomena (vortex = 78, difluence = 47, confluence = 39, saddles = 35). The training set corresponds to remaining simulation 4D data with annotations from four months (vortex = 140, difluence = 119, confluence = 193, saddles = 142). The performance measure used to evaluate the classification was the average accuracy, i.e. the average of the accuracy per class.

For parameter selection, a stratified 5-fold cross-validation scheme was applied over the training dataset for each strategy (combinations of features and classifiers). The same folds distribution was used for all strategies in order to compare them in the same conditions. The parameter combination that obtained the best performance was used to train a model using the whole training dataset. The final performance measure was reported over the independent testing dataset for each strategy for comparison.

The representations evaluated were defined as follows: *pyrHOOF* (baseline) by concatenating the HOOF descriptor for each region obtained from SPL, *histdivcurl* is the concatenation of histogram distribution of the three feature maps of atmospheric operators (curl, divergence and negative divergence), *pyrdivcurl* is the histogram concatenation of the three feature maps for each region obtained from SPL, and *maxpooldivcurl* is the corresponding histogram obtained by applying max-pooling over all concatenated histograms from regions obtained from the SPL.

3.3 Results

Table 1 shows the classification performance of the proposed method evaluated in terms of accuracy for the different representations and classification methods. Notice that these results were obtained from independent data corresponding to a month of simulation. The best performance measure was achieved by the complete SPL representation without max-pooling (*pyrdivcurl*) and using a Support Vector Machine with an RBF kernel obtaining an average accuracy of 0.81. In general, the confluence class shows the highest accuracy for the most configurations whereas saddle point class have the worst performance. Interestingly max-pooling applied over SPL does not help because most of the region annotations are centered in the atmospheric structure. However, preliminary work with larger regions where the atmospheric structure was not at the center, the max-pooling over SPL obtained the best results. Table 1 also shows that performance achieved using SVM with a linear kernel is very close to the reported one using SVM with RBF kernel. Furthermore Random Forest classifiers were trained with 10,000 estimators, indeed during cross validation we could determine that increasing the number of estimators did not improve our results.

Table 1. Classification performance in test dataset in terms of accuracy.

Feature	Classifier	Vortex	Difluence	Confluence	Saddle pt	Avg. Accuracy
pyrdivcurl	SVM-RBF	0.71	0.82	0.92	0.77	0.81
histdivcurl	SVM-RBF	0.69	0.87	0.89	0.6	0.765
maxpooldivcurl	SVM-RBF	0.69	0.87	0.89	0.6	0.765
pyrHOOF	SVM-RBF	0.76	0.87	0.56	0.48	0.672
pyrdivcurl	SVM-Linear	0.74	0.8	0.92	0.71	0.797
histdivcurl	SVM-Linear	0.75	0.78	0.87	0.6	0.753
maxpooldivcurl	SVM-Linear	0.75	0.78	0.87	0.6	0.753
pyrdivcurl	RF	0.73	0.8	0.94	0.6	0.771
maxpooldivcurl	RF	0.69	0.85	0.92	0.51	0.745
histdivcurl	RF	0.69	0.85	0.92	0.45	0.73
pyrHOOF	RF	0.62	0.97	0.58	0.34	0.634

4 Concluding Remarks

This paper presents a successful application of a novel method which combines features based on differential operators and machine learning classifiers to discriminate *low level* wind structures. The feature maps obtained from approximate differential operators help to highlight the relevant atmospheric structures. The SPL show the best classification performance since it includes multi–resolution information, despite the complexity of the structures.

Future work includes to increase the dataset with more annotations of *low level* and new *high level* atmospheric structures, adding more atmospheric variables, enhancing the *low level* structure characterization, as well as to develop a detection method to efficiently analyze whole 4D volumes.

Acknowledgments. This work was funded by project number 1225-569-34920 "*Diseño e implementación de un sistema de cómputo sobre recursos heterogéneos para la identificación de estructuras atmosféricas en predicción climatológica*" through Administrative Department of Science, Technology and Innovation of Colombia (Colciencias). We want to thank Diana Díaz and Darwin Martínez for their valuable hints and discussions.

References

1. Armenta, G., Pabón, J.: Modeling northern South America and Caribbean climate using PRECIS and WRF for climate variability and change studies. In: Proceedings of the CORDEX-LAC1 Workshop - World Climate Research Programme, Lima, Peru (2013)
2. Chaudhry, R., Ravichandran, A., Hager, G., Vidal, R.: Histograms of oriented optical flow and Binet-Cauchy kernels on nonlinear dynamical systems for the recognition of human actions. In: IEEE Conference on Computer Vision and Pattern Recognition, CVPR 2009, pp. 1932–1939, June 2009
3. Gruchalla, K., Rast, M., Bradley, E., Clyne, J., Mininni, P.: Visualization-driven structural and statistical analysis of turbulent flows. In: Adams, N.M., Robardet, C., Siebes, A., Boulicaut, J.-F. (eds.) IDA 2009. LNCS, vol. 5772, pp. 321–332. Springer, Heidelberg (2009)
4. Holmén, V.: Methods for vortex identification. Master's thesis, Lund University (2012)
5. Lazebnik, S., Schmid, C., Ponce, J.: Beyond bags of features: spatial pyramid matching for recognizing natural scene categories. In: 2006 IEEE Computer Society Conference on Computer Vision and Pattern Recognition, vol. 2, pp. 2169–2178 (2006)
6. Michalakes, J., Chen, S., Dudhia, J., Hart, L., Klemp, J., Middlecoff, J., Skamarock, W.: Development of a next generation regional weather research and forecast model. In: Developments in Teracomputing: Proceedings of the Ninth ECMWF Workshop on the Use of High Performance Computing in Meteorology, vol. 1, pp. 269–276. World Scientific (2001)
7. Murphy, A.H.: What is a good forecast? an essay on the nature of goodness in weather forecasting. Weather and Forecasting **8**(2), 281–293 (1993)
8. Nagi, J., Ducatelle, F., Di Caro, G., Ciresan, D., Meier, U., Giusti, A., Nagi, F., Schmidhuber, J., Gambardella, L.: Max-pooling convolutional neural networks for vision-based hand gesture recognition. In: 2011 IEEE International Conference on Signal and Image Processing Applications (ICSIPA), pp. 342–347, November 2011
9. Rao, A.R., Jain, R.C.: Computerized flow field analysis: Oriented texture fields. IEEE Transactions on Pattern Analysis and Machine Intelligence **14**(7), 693–709 (1992)
10. Tzeng, F.Y., Ma, K.L.: Intelligent feature extraction and tracking for visualizing large-scale 4d flow simulations. In: Proceedings of the 2005 ACM/IEEE Conference on Supercomputing, p. 6. IEEE Computer Society (2005)